Available online at www.sciencedirect.com
ScienceDirect
Journal of Geochemical Exploration 98 (2008) 116–128
JOURNAL OF GEOCHEMICAL EXPLORATION
www.elsevier.com/locate/jgeoexp

Usefulness of geological, mineralogical, chemical and chemometric analytical techniques in exploitation and profitability studies of iron mines and their associated elements

M. Dolores Petit-Dominguez [a,*], M. Isabel Rucandio [b], Almudena Galan-Saulnier [c], Rosario Garcia-Gimenez [d]

[a] Departamento de Química Analítica y Análisis Instrumental, Facultad de Ciencias, Universidad Autónoma de Madrid, E-28049-Madrid, Spain
[b] Madrid, Spain
[c] Departamento de Arquitectura y Tecnología de Sistemas Informáticos, Facultad de Informática, Universidad Politécnica de Madrid, Madrid, Spain
[d] Departamento de Geología y Geoquímica, Facultad de Ciencias, Universidad Autónoma de Madrid, E-28049-Madrid, Spain

Received 11 October 2007; accepted 10 January 2008
Available online 4 February 2008

Abstract

Due to the high number of variables involved in mine profitability studies, it is often very difficult to establish connections among them in order to provide a blend of market saleable quality products. In this sense, analytical chemistry together with chemometry are essential and indispensable disciplines to tackle these studies. The aim of this work was to demonstrate the utility of these disciplines to carry out optimization studies of iron mines. For this purpose, one of the most important iron mines of the Iberian Peninsula was chosen, sited in the mountain range of Sierra Menera, near the location of Ojos Negros (Teruel, Spain). Geological, mineralogical and chemical composition of 148 samples was analyzed, corresponding to different depths of three drill holes (named TE1, TE2 and TE3). In particular, aspects concerning to chemical composition are very important, since the mean contents of certain elements, such as phosphorus, sodium and potassium, should be restricted to the established limits to prevent that companies can drive back the raw material if they do not fulfil the necessary requirements. On the other hand, the large number of analysed samples drove us to use a statistical processing of the data. Among other aspects, it provides a way to find possible connections among a high number of variables and classify samples into compositional groups sharing similar composition, in order to limit the mineralised area and to obtain enough information about the amount of those chemical elements associated to iron ores. Data obtained from all these analytical techniques were in good agreement and provide a methodology that can be of wide interest applied to different geological studies.
© 2008 Elsevier B.V. All rights reserved.

Keywords: Iron ores; Phosphorus; Sodium; Potassium; Analytical techniques

1. Introduction

Iron is the fourth element more abundant in the nature. Its deposits are known from antiquity and they have been used in numerous applications. In this sense, Spain has been one of the word leading iron producers during the last part of the 19th and the first quarter of the 20th centuries (Zitzman and Neumann Redlin, 1976) and even nowadays, has abundant reserves of this element.

Several aspects must be taken into account to consider an iron deposit economically profitable, such as appropriate volumetric measurement, mineralogical and chemical composition, physical composition relating to the grain size and geographical location. In particular, aspects concerning to chemical composition are very important, since the mean contents of certain elements should be restricted to the established limits to prevent that companies can drive back the raw material if they do not fulfil the necessary requirements. Among these elements, the presence of phosphorus above a determined level increases the fragility of iron and steel products and forces the election of a particular industrial process. Then, there is a general trend to

* Corresponding author. Fax: +34 914974931.
E-mail address: mdolores.petit@uam.es (M.D. Petit-Dominguez).

0375-6742/$ - see front matter © 2008 Elsevier B.V. All rights reserved.
doi:10.1016/j.gexplo.2008.01.003

reduce costs avoiding the employment of mineralizations with high phosphorus contents. An iron mineral with a phosphorus content above 0.15% expressed as the corresponding oxide is normally driven back. Phosphorus could be also a problem if it is solubilised, since it could cause ecological impacts in surface waters (Haygarth, 2005, Haygarth et al., 2005). On the other hand, alkaline elements (sodium and potassium) produce complex carbonates, which are deposited in the refractory materials affecting the normal function of the blast furnace. In these cases, the maximum contents accepted by the different companies use to be between 0.22 and 0.45% expressed as K_2O+Na_2O.

Due to the high number of variables involved in mine profitability studies, it is often very difficult to establish connections among them in order to provide a blend of market saleable quality products. In this sense, analytical chemistry together with chemometry are essential and indispensable disciplines to tackle these studies.

The aim of this work was to demonstrate the utility of these disciplines to carry out optimization studies of iron mines that can be extended to other different studies in the chemical and geological fields. For this purpose, one of the most important iron mines of the Iberian Peninsula during the twenty century was chosen (Fernández-Nieto, 1977), sited in the mountain range of Sierra Menera, near the location of Ojos Negros (Teruel, Spain). Geological, mineralogical and chemical composition of 148 samples was analyzed, corresponding to different depths of three drill holes (named TE1, TE2 and TE3).

Geological and mineralogical analyses helped us to establish the lithologic columns of the drill holes and to know their vertical mineralogical composition respectively. In addition, mineralogical data were displaying using a Box and Whisker plot, a histogram-like method that helps us to interpret the distribution of data, and statistical and chemometrical analysis of them were carried out.

Chemical analyses allowed us to know the major constituents, as well as the contents of phosphorous and alkaline elements, according to the different zones, previously defined for each drill hole from a mineralogical point of view. Besides, the large number of samples analysed drove us to use statistical processing of the data. In this sense, correlations among the analytical variables were calculated considering in some cases all samples and in others those from the mineralised areas. Cluster analysis was carried out to establish groups of chemical and mineralogical parameters with similar characteristic. Supervised Pattern Recognition was applied in this study to those 71 samples corresponding to mineralised areas of TE1, TE2 and TE3 drill holes, considering the 8 chemical parameters as variables (Fe_2O_3, MnO, Al_2O_3, CaO, MgO, Na_2O, K_2O and P_2O_5). Discriminant analysis was used for hard classification, which provides a way to find possible connections among a high number of variables and classify samples into compositional groups sharing similar composition, in order to limit the mineralised area and to obtain enough information about the amount of those chemical elements associated to iron ores.

Finally, in a group of selected samples, observations made by polarization microscopy and scanning electron microscopy (SEM) equipped with an energy dispersive X-ray (EDX) analyzer, allowed us to distinguish and to classify different material types in relation to their texture and mineral composition.

2. Geological setting, mineralization and mining

The Ojos Negros mine complex is sited at a height of 1500 m.a.s.l. in the mountain range of Sierra Menera (NE of Spain, Fig. 1A). This mountain range is located from N-NE to S-SW direction and it constitutes the border between Teruel and Guadalajara provinces (Spain) (Fig. 1B).

2.1. Structure and stratigraphy

The ore body Tío Elías (Fig. 1C) is located in the slope NE of the Sierra Menera in the Ojos Negros mine complex near the foothills of Alto del Vicario, limited by Navarrosa sector and separately by a big break. The ore body is formed by strata-bound, surrounded with the sandstone and quartzite from the roof and walls. In the sides the croup out have faults (Fernández Rubio, 1976). The thickness of the orebodies is typically from less than 1 up to 10 m.

Topographically, it is also the watershed (Pico Lobo, 1538 m. a.s.l), in the eastern slope is sited the Ebro river basin and in the western slope the Tajo river one.

The basal portion of the stratigraphic sequence consists of quartzite and graywacke of Early Ordovician age with intercalations of sandstone and iron oolitic layers (Herranz et al., 2003). It is overlaid by a Late Ordovician carbonate dominated succession, known as the Pobo limestone (Villena, 1976) which are divided into three members: (i) quartzite and sandstone with silty intercalations, (ii) an irregularly distributed sequence of marble, shale and carbonate (Cabezo limestone) including Mg–Fe carbonates and (iii) dolostone, iron oxides and hydroxides and clays (Fig. 1C).

From the structural point of view, the Hercynian basement is composed of Precambrian to Permian rocks with preferred N–NW to S–SE directions (Fernández-Nieto et al., 1981). The intracratonic Iberian basin was developed during the Alpine orogeny (Tertiary) and initially filled by fluviatile clastic sequences.

2.2. Mineralization

Sierra Menera is a Paleozoic massif composed by goethite gossans formed from weathering processes (Villena, 1976). It is hosted by Ordovician and Silurian basement rocks (western of Iberian Range).

The strata-bound ore bodies are preferentially located on the flanks of Sierra Menera anticline. The Paleozoic strip is extended to the Almohaja (South) and Pobo de Dueñas (North) where several massifs crop out with about 35 Km long and 10 Km mean wide (Villena, 1976; Fernández-Nieto, 1977; Fernández Nieto and Arrese, 1979; Fernández Nieto et al., 1981, 2003). They are mainly composed of Mg–Fe carbonates (belonging to sideritemagnesite series) and dolomite, with a gangue of quartz, clay minerals and calcite. Mg–Fe carbonates at Sierra Menera occur as

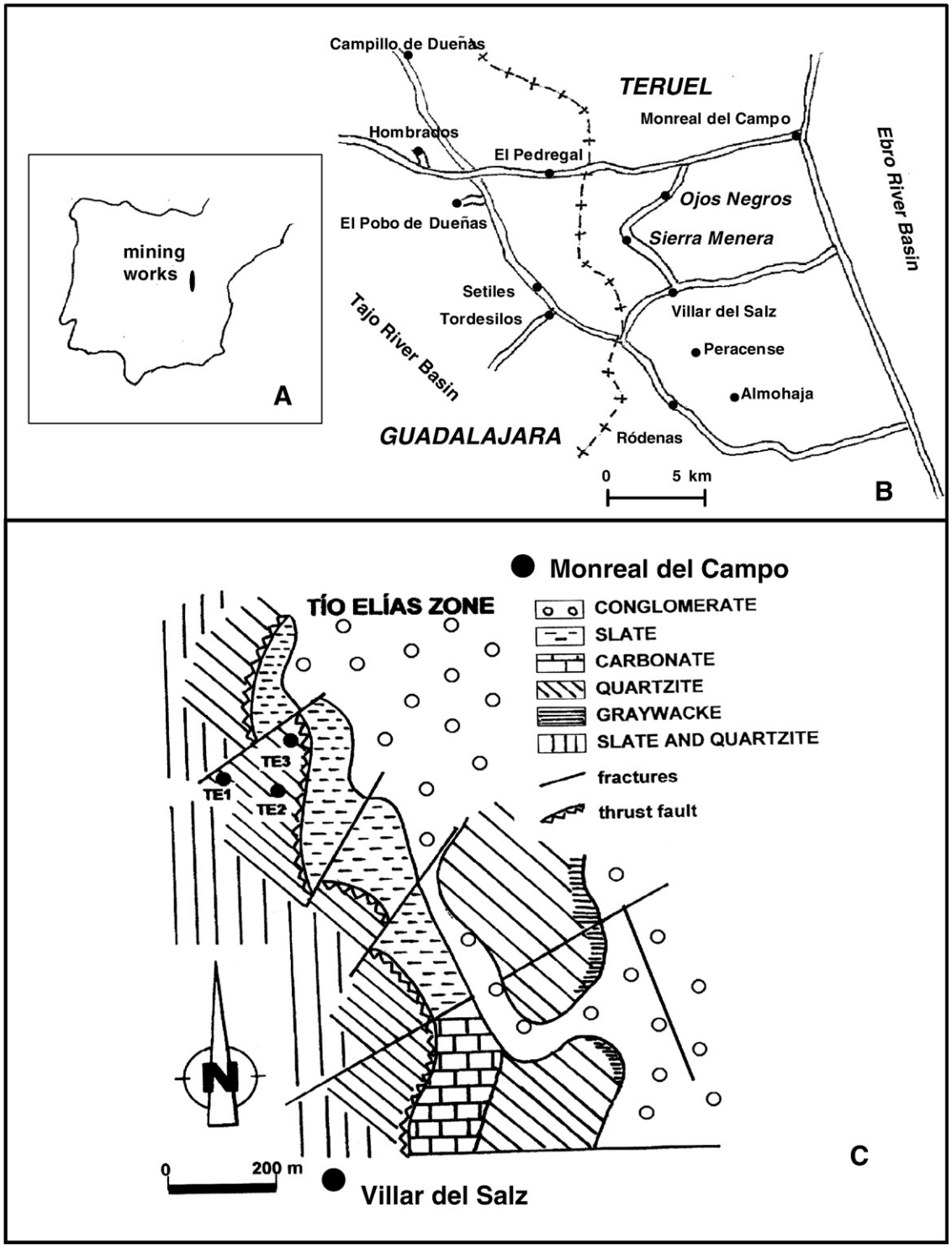

Fig. 1. Location map (A, B) and geological distribution (C).

lenticular to irregular ore bodies, with are interfingered with the host dolostone. The massive dolomites are foregoing by green slates or fossiliferous marges. In the top of sequence there is an erosive discontinuity or an open paleokarst with ferruginous packed. The upper part of the Mg–Fe carbonate bodies was affected by oxidation processes linked to late Pliocene karstification, which gave rise to goethite gossans.

2.3. Mining

Mining activities in the Tío Elías zone began in 1985 with resources of about five million metric tonnes.

The ore District is distributed in the villages: Campillo de Dueñas, Hombrados, El Pobo de Dueñas, El Pedregal, Setiles, Tordesilos and Ródenas (Guadalajara) and Ojos Negros, Villar

del Salz, Peracense and Almohaja (Teruel) (Fig. 1B). This area is located in the central part of the Iberian Mountain Chain, in the called Rama Castellana or Celtiberics Chains, which consists of small Mesozoic massifs cored by a Paleozoic basement and separated by basins filled by detrital rocks during the Tertiary and Quaternary periods.

3. Sampling and methods

3.1. Drill hole sampling

Sampling was carried out in the area called Tío Elías. The ore body was according with the sandstone and quartzite from the surroundings. Materials have a low crystalline grade. They are much hydrated and plenty of holes, showing recent deposits (Urquiza et al., 1985). A sampling campaign was made with eight mechanic drillings in order to limit the mineralised area. A bore B-50 in continuous wined (one sample/one meter) was used except in the sterile zone where samples were collected at different depths. Three drill holes were selected to illustrate this work (Fig. 1C). One of them presented a high volume of iron ore and the other two were useful to study the surrounding materials. A total of 148 samples corresponding to different depths of three drill holes (TE1, TE2 and TE3) were analysed.

The collected samples were dried in an oven at 110 °C and then ground and particle homogenized by using an agate mortar and a ball grinder until reaching a particle size lower than 74 μm.

3.2. Mineralogical analysis

The mineralogical composition were analyzed by X-Ray Diffractometry (XRD) (Schultz, 1964; Barahona, 1974; Brindley, 1980) using a Siemens D-5000 diffractometer with a tungsten cathode and iron anode operating at 30 mA and 40 kV. Randomly orientated specimens were continuously scanned in the range 3–65° 2θ at the rate of 2°/min, using 0.18 and 1° as entrance and divergence slits respectively. X-ray diffraction patterns were obtained and peak positions (d-spacing) were determined using the Siemens software.

3.3. Chemical analysis

Samples were digested with a treatment based in a conventional heating wet decomposition (Papadopoulou et al., 2004; García Giménez et al., 2006) with some modifications: 0.1 g of homogenized sample was treated two hours in closed vessels at 130–160 °C with a mixture of 4 mL aqua regia and 2 mL concentrated hydrofluoric acid. 10 mL of saturated boric acid solution was added to the obtained solution and it was diluted to 25 mL with water. Al, Ca, Fe, Mg and Mn were determined by Flame Atomic Absorption Spectrometry (FAAS), using a Perkin Elmer 503 spectrometer, while Na and K by Flame Atomic Emission Spectroscopy in a Cornning EEL spectrometer.

Standard solutions were made from 1 g L^{-1} (weighed to ± 0.1 mg) stock solutions (Merck, Darmstadt). Blank assays with reagents were found to be negligible. For QA/QC, standards including NIST Standard Reference Materials (2710 Montana Soil and 2709 San Joaquin Soil) and Standard References of Iron Ores (NBS 690 and 693) were analysed together with the samples. Six replicate analyses of some selected samples and standards showed a precision of typically less than 7% (coefficient of variation) for the analysed elements.

3.3.1. Phosphorus determination

Two types of determination procedures were carried out in order to determine the phosphorus content in the samples by visible spectrophotometry:

When the phosphorus contents were lower than 0.05%, 1 g of sample (weighed to ±0.1 mg) was treated with 30 mL (1+1) nitric acid and heated until nitrous vapours appeared. Then 10 mL of 2.5% potassium permanganate and 10 mL hydrogen peroxide were added to obtain a colourless liquid. Finally 10 mL ammonium vanadate was added and the solution heated to boiling and filtered through a 238 paper filter. The obtained solution was poured into a 100 mL volumetric flask containing 10 mL 5% ammonium molybdate solution. It was left to cool down, diluted to the mark and analysed. The yellow complex formed is measured at 430 nm.

In samples with phosphorus contents higher than 0.05%, 1 g of sample (weighed to ±0.1 mg) was treated with a mixture of 25 mL perchloric acid, 18 mL nitric acid and 7 mL hydrochloric acid and heated until perchloric vapours were obtained. Solution was filtered through 242 paper filter and diluted to the mark in 1000 mL volumetric flask. An aliquot of 10 mL of this solution was taken and treated with 10 mL sulphurous acid in a boiling water bath. After cool, 10 mL bismuth nitrate, 10 mL 2% sodium molybdate and 2 mL ascorbic acid were added. It was diluted to the mark in 100 mL volumetric flask and the blue complex formed measured at 725 nm.

For both methods, a standard solution of 1 g L^{-1} (weighed to ±0.1 mg) of phosphorus was prepared by dissolution of potassiumdihydrogenphosphate in water. Aliquots of this solution was taken and treated in the same way that samples in order to prepare the corresponding calibration curve (Jackson, 1976). All measurements were referred to a corresponding blank solution.

3.4. Microscopical analysis

Transversal thin sections of the samples (20–25 μm) were cut off. When adequate thin sections of samples were not possible to obtain, the samples were consolidated with resin (cronolite) and cut off after drying as described. Mineral components and paste texture were observed using a Petrographic Polarisation Orto Plan Pol Leitz Microscope. In addition, observations of 1 μm layers corresponding to some samples, polished with diamond, were made by Scanning Electron Microscopy (SEM) using a Carl Zeiss 500E microscope and quantified with an Energy Dispersive X-Ray (EDX) analyzer.

3.5. Statistical and chemometrical analysis

A statistical processing of the data was carried out using the SPSS 1.5 and STATGRAPHICS Plus 5.0 for Windows®. Correlations among the analytical variables were calculated

considering in some cases all the samples and in others those from the mineralised areas. Cluster and multivariate statistical analyses were performed by using chemical and mineralogical data of the 71 studied samples from the mineralised areas of TE1, TE2 and TE3 drill holes.

Cluster analysis was carried out to establish groups of chemical or mineralogical parameters with similar characteristics. Supervised Pattern Recognition was applied in this study to those 71 samples, considering the major constituents as variables: 9 mineralogical parameters and 8 chemical parameters. Discriminant Analysis was used for hard classification purposes, trying to establish possible connections among groups of samples and variables (García Giménez et al., 2005; Marini et al., 2004). This procedure is useful for classifying the dataset into groups according to the location of the different drill holes. It generates a small number of functions of quantitative measurements which are linear combinations of the standardized pattern variables with weight coefficients. These functions are called Canonical Discriminant Functions and help to discriminate among groups of samples. The procedure assumes that the variables are drawn from population with multivariate normal distributions and that variables have equal variances.

4. Results and discussion

4.1. Geological and mineralogical composition

Geological and mineralogical results were obtained from the observation and mineralogical analysis by X-Ray Diffractometry. This technique is very useful for qualitative and semiquantitative analyses of the crystalline phases, but quantitative analyses provide less accurate results than chemical analyses and they are limited to the crystalline forms. These semiquantitative results are adequate for comparison of samples and areas. From these results, geological and mineralogical compositions of the three drill holes are shown in Figs. 2 and 3. Fig. 2 represents geological composition, remarking the principal component of each depth and Fig. 3 shows graphics of the mineralogical composition, including the most important crystalline phases.

4.1.1. Lithology

The drill hole number TE1 was sited in the western zone (Fig. 1C). It is well mineralized with a depth of 119 m, showing three different zones. The first 56 m were composed by fine grains of quartzite in shades from grey to yellow-reddish. Dispersed micaceous layers were detected with intercalations of grey slate. The mineralized zone (56–111 m) was in a red colour due to the presence of powdered iron materials with diverse compact degrees. It could be detected the presence of goethite, hematite, quartz, carbonates (calcite, dolomite and magnesite) and traces of phyllosilicates. Finally, the other zones were formed by two lithologies. One of them was above the mineralization. It was formed by slate, quartz (60%) and muscovite (well crystallised). The second one, located at the bottom, was a dark pelitic zone with a decrease of the iron ore and a high level of micaceous minerals, quartz, dolomite, siderite and goethite.

The drill hole number TE2, with 111 m of depth, was located at the eastern of TE1. It is the drill hole with a minor mineralization.

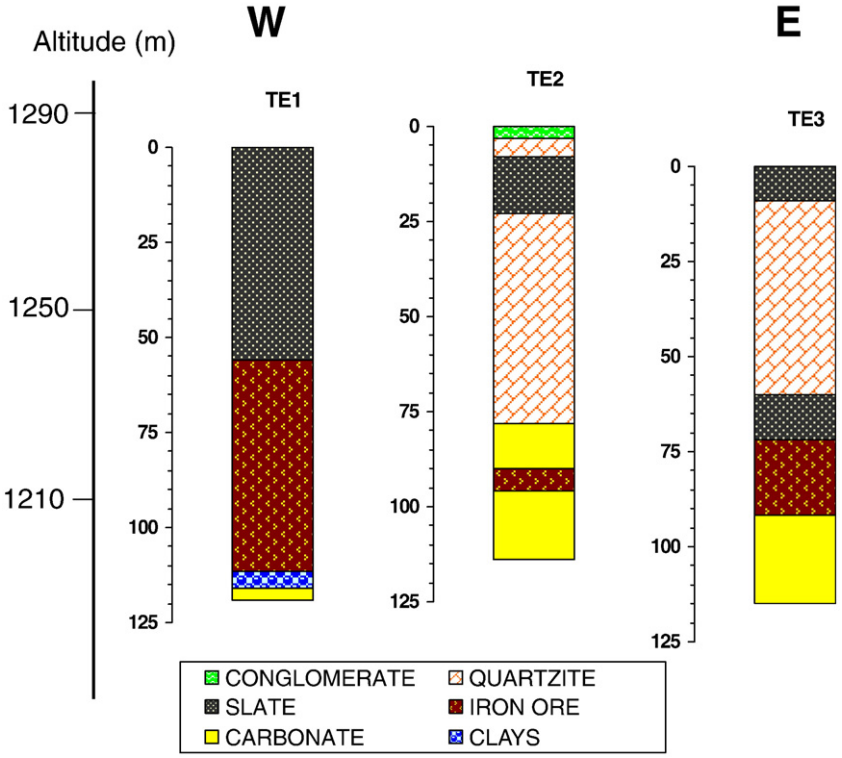

Fig. 2. Lithologic columns of the drill holes.

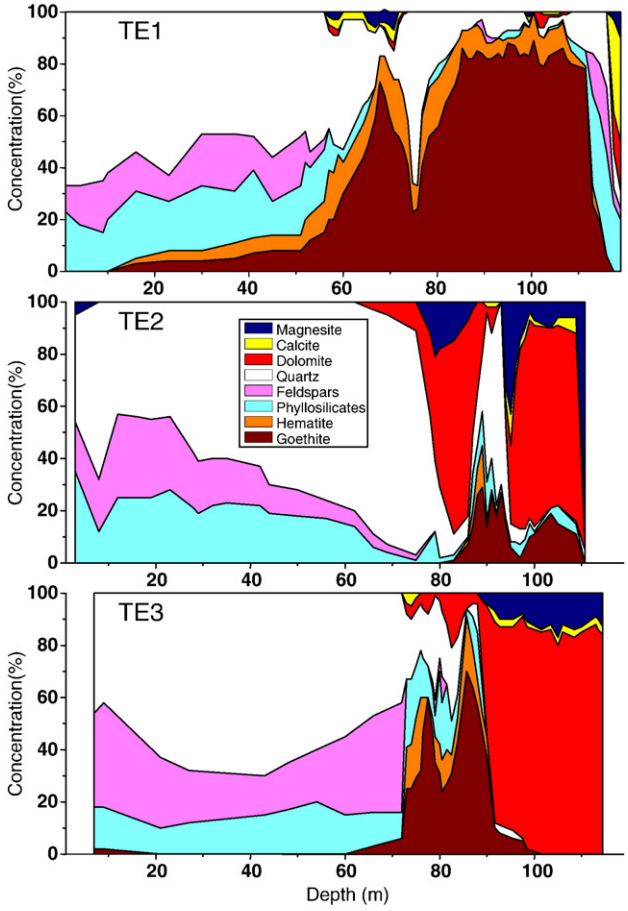

Fig. 3. Vertical mineralogical distribution.

The first 23 m were compact and greasy and they were composed by black slate. The second length (52 m) was composed by medium-to thick-grain quartzite with eventual slate. At the bottom of the drill hole it could be distinguish three parts: an upper zone composed by quartz and carbonates (magnesite and dolomite), an intermediate zone where quartz, goethite, hematite an iron–magnesium carbonates were detected and finally, a dolomitic zone with goethite. The mineralization appears as irregular veins, granular aggregates or impregnations in rocks.

The last drill hole (number TE3) with 115 m of depth was located at the north of the drill hole number TE2. The first length (70 m) was composed by compact quartzite of thick grains in grey-white to yellow tones with eventual slate beds. In the second length (45 m) iron ores in shades of red were presented with quartz and phyllosilicates increasing the dolomitic materials with the depth.

4.1.2. Vertical mineralogical distribution

Fig. 3 represents the distribution in depth of the different crystalline phases for the three drill holes. These data show a radical change in the composition at about 80 m for TE2 and 72 m for TE3, with a noticeable increment in dolomite concentration at a higher depth. The mineralized areas of these two drill holes were found close to the changing area. On the contrary, the mineralized area of TE1 is broader, covering about 50 m deep, with high level of iron ore. The mineralogical composition of the zones above the mineralized area in the three drill holes are composed mainly by quartz, phyllosilicates and feldspars.

4.1.3. Statistical and chemometrical analysis

Pearson product moment correlations among variables were calculated considering the different crystalline phases as variables. The correlation coefficients measure the strength of the linear relationship between the variables. The correlation coefficients obtained for the total number of considered samples are relatively low (<0.55). This fact means that there are not crystalline phases associated to others; that is, each one has a different behaviour.

On the other hand, the cluster analysis for the mineral contents of mineralized area samples coming from TE1 drill hole was obtained. This procedure has created 1 cluster from the 8 crystalline phases supplied. The clusters are groups of observations (crystalline phases) with similar characteristics. To form the clusters, the procedure began with each crystalline phase in a separate group. It then combined the two observations which were closest together to form a new group. After recomputing the distance between the groups, the two groups then closest together were combined. This process was repeated until only 1 group remained. In this case (Fig. 4A), goethite creates a group

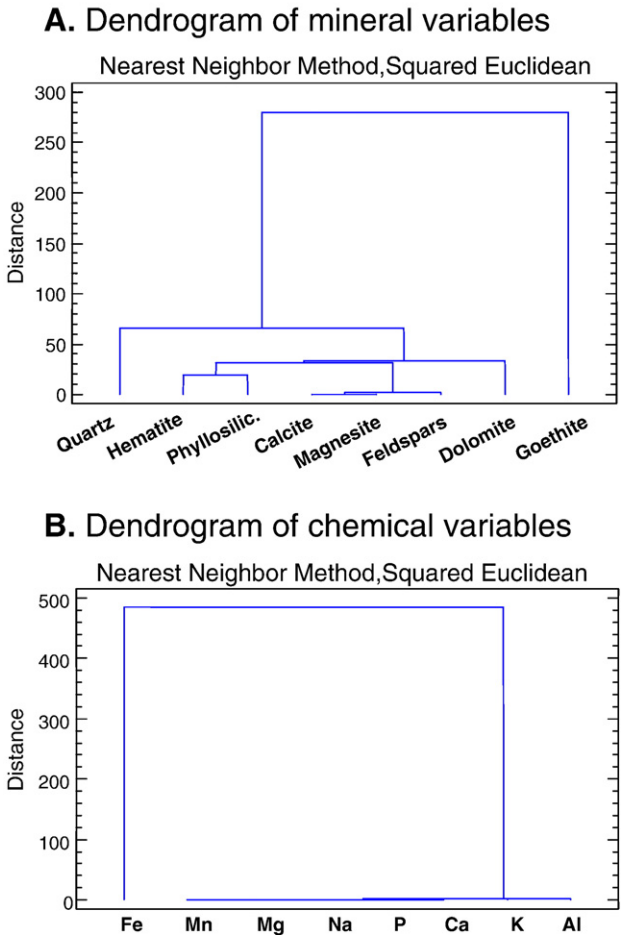

Fig. 4. Cluster analysis of the A. Chemical cases and B. Mineral cases.

clearly separated to the rest crystalline phases, more similar among them. Mineral composition of mineralised area was very uniform, formed by goethite in different recrystallization degrees. In this way, globular aggregates formed by limonite (goethite and hematite) are less stable than goethite, which is the most stable mineral. Other components dispersed in the globular mass, such as Si and Mn are ordered in other more stable crystalline phases. In any case goethite is the component that governed the stabilization of the system, in relation or not to carbonates and silicates (all of them stable phases), and against the other less stable crystalline phases.

Fig. 5 represents Box and Whisker plots for mineral components in all samples of the mineralised areas. In these plots each box encloses the middle 50%, where the median is represented as a horizontal line inside the box. Vertical lines extended from each end of the box (called whiskers) enclosed data within 1.5 interquartile ranges. Values than fall beyond whiskers, but within 3 interquartile ranges (suspect outliers), are plotted as individual points (○). Far outside points (outliers) are distinguished by special character (*). Box and Whisker plot shows in general a low symmetry distribution of data. From a simple observation of the graphic, it is very easy to compare the mineral composition of the different drill holes taking into account as average values as the dispersion of the data and the outliers. In this sense, most important differences are observed in the major constituents: goethite and quartz. It is remarkable the high level of goethite in TE1 and quartz in TE2. In a different scale, the rest of the components are represented. Dolomite shows high and dispersed values for TE2, as a consequence of a limited number of samples analysed in the small mineralised area (6 m) and their high compositional variability. On the other hand, dolomite content in mineralised area of TE1 (45 samples and 55 m) is much lower with a minor dispersion.

4.2. Chemical composition

4.2.1. Major constituents

Al, Ca, Fe, Mg and Mn were quantitatively determined in the 148 selected samples by Flame Atomic Absorption Spectrometry and Na and K by Flame Atomic Emission Spectrometry. Standard Reference Materials where analysed in a similar way for two types of materials: NIST 2710 and NIST 2709 for soils and NBS 690 and NBS 693 for iron ores. The obtained results agree with all certificate values with errors lower than 5%. The data deduced for the 148 samples, expressed as percentages of their respective oxides, are represented in Fig. 6. The results reveal a large extension in TE1 (56–111 m) of abundant presence of iron ore. In this figure could be distinguish for each drill hole the different zones according with the already defined from a mineralogical point of view.

Considering the iron ore length, the highest mean percentage in the iron content (61.7%) was found in TE1, with a maximum value of 75.1%, followed by TE 3 (51.0%) with a maximum value of 64.3%, being TE2 the least mineralised with average content of iron about 40.2% and maximum value of 56.3%. TE1 was the drill hole with a higher grade of mineralization, but at the same time presents the highest amounts of Na, K and P associated to the iron ore. It is remarkable the amount of K (1.70%) with a maximum value of 26.0% compared with the other ones (TE2 with an average value of 0.047% and maximum value of 0.090% and TE3 with an average value of 0.035% and maximum value of 0.060%). TE1 also showed the highest average values for Mn and Ca. TE2 has the highest average values for Al and TE3 for Mg and similar average value for P (0.085%) than TE1 (0.087%).

In the length above iron ore, it is remarkable the higher amounts of Al (18.4%) and K (0.70%) in TE1, Ca (4.99%) and Mg (3.68%) in TE2 as well as the lower amounts of Fe (2.43%), Mn (0.08%), Na (0.013%) and K (0.031%) in TE3.

In the length under the iron ore, it is noticeable the higher amounts of Al (20.0%), Na (0.54%), K (0.91%) and P (0.036%) in TE1, Ca in TE2 and TE3 with average values of 20.0 and 26.0%, respectively.

These zones were chemically classified and a summary of the obtained results for the analysed chemical elements are shown in Table 1. In this table the means, the standard deviations and the extreme values for each zone of every drill holes were calculated. These data reveal high values of Fe in the

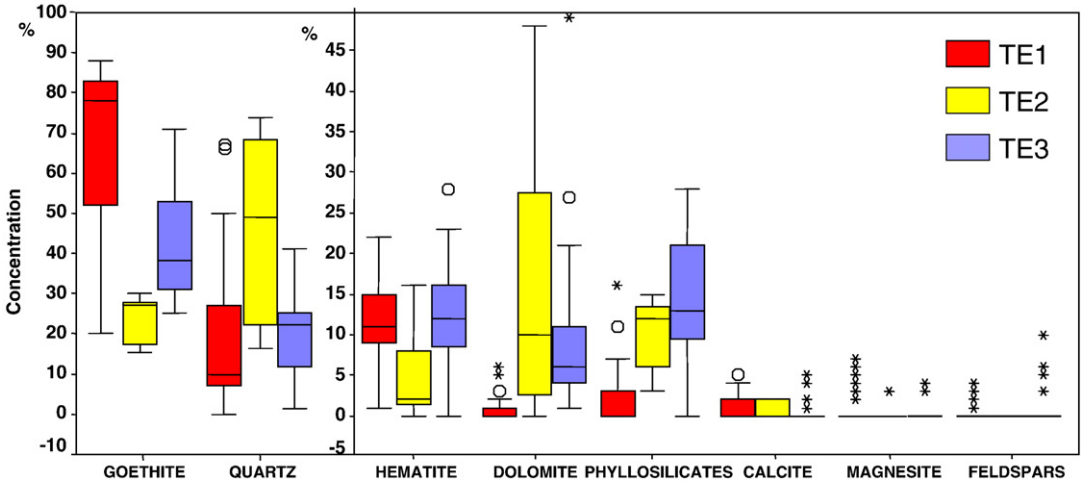

Fig. 5. Box and Whisker plot of the mineralogical components.

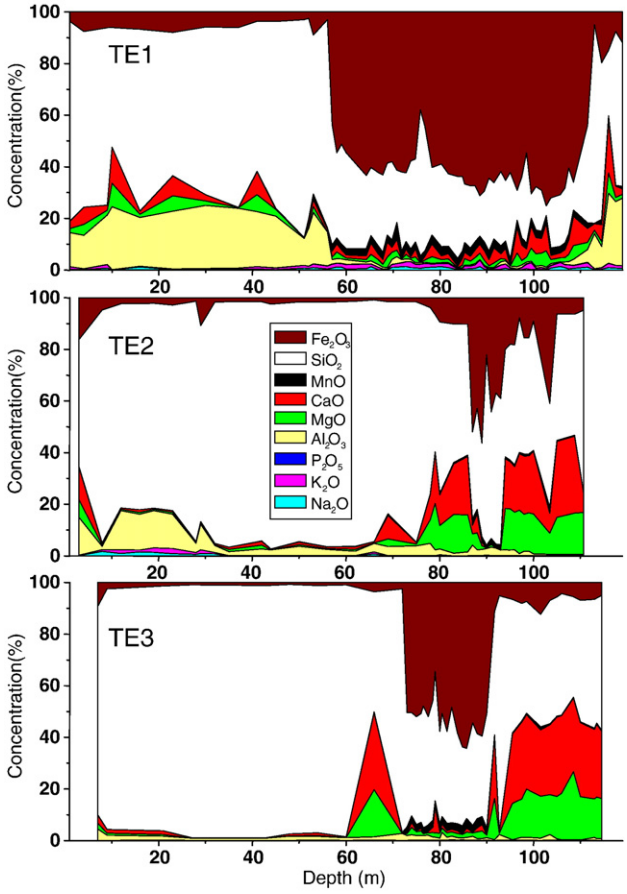

Fig. 6. Vertical chemical distribution.

intermediate area of each drill hole, as well as, the associated elements such as Mn. Important differences were observed for Al_2O_3 content, being higher in TE1 as a consequence of the presence of phyllosilicates. Mean values for TE2 and TE3 in the non-mineralised zones were 1–6 and 0.8–1.8, respectively.

CaO and MgO results show a noticeable increase from the upper areas to the lowest ones, mainly in TE2 and TE3. This is due to the presence of carbonated minerals such as dolomite, magnesite and calcite below the mineralization area. TE1 also has a carbonated area with high level of calcite at the bottom, but the presence of clays in the proximities of the mineralisation and the fact that only 5 samples were taken in these area make these results are not enough to extract conclusions.

4.2.2. Alkaline elements

The level of alkaline elements could be classified in two groups. One of them with values ranged between 0.4 and 0.9% expressed as oxides, and the others with values lower than 0.05%.

The samples in the first group are in TE1 and the upper area of TE2, whereas those of the second group are composed by samples of TE3 and the mineralization and lower areas of TE2. Generally and at first sight, it seems to be in relation to the presence of phyllosilicates and feldspars, but in some cases those minerals are not associated with these elements, but a more detailed study reveals that Na and K are in a close relation to micaceous minerals from slates like muscovite and paragonite, and in a minor proportion, with feldspars associated to quartzite.

4.2.3. Phosphorus

Phosphorus is an element of hard determination by Flame Spectrometry due to its low absorption and emission wavelength. It requires the employ of argon or nitrogen gas to avoid the absorption of this radiation by the present oxygen. In this sense, Hoft et al., 1979 used Flame Atomic Absorption Spectrometry with nitrous oxide-acetylene flame for phosphorus determination. Also other instrumental techniques were applied directly to solid samples by X-ray Fluorescence Spectrometry (Pereira and Brandao, 2001) or to liquid samples by using Inductively Coupled Plasma Atomic Emission Spectrometry (Kirkbright et al, 1972). In this work, other alternative analytical methods based on visible spectrophotometry were considered for the indirect determination of phosphorus.

Since phosphorus has a large affinity by clay minerals, an energetic attack is required to put it into solution. Two methods were selected as a function of the availability of the equipment and reagents, the dissolution procedure and the phosphorus content. They were described in the phosphorus determination section. Both methods agree in their results when phosphorus contents are about 0.05%.

From the obtained results, it can be concluded that phosphorus contents are significantly higher in the mineralised area although there are a great dispersion in these results. As it was said above, TE 1 was the drill hole with a higher grade of mineralization, but at the same time presents the highest amounts of P associated to the iron ore.

4.2.4. Statistical and chemometrical analysis

A study of the correlation between pair of variables was carried out in a similar way than that for the mineralogical parameters. The 8 chemical element concentrations were considered as variables (Fe, Mn, Al, Ca, Mg, Na, K and P), and concentrations were introduced as percentages of their respective oxides. The following pair of variables has *P*-values below 0.05 indicating statistically significant non-zero correlations at the 95% confidence level: Fe and Mn, Fe and Ca, Fe and Mg, Ca and Mg, Ca and K. All of these correlations, with exception of the last one, were significant at 0.01 levels. The similar behaviour between Fe and Mn ($r=0.567$) or Ca and Mg ($r=0.792$) is predictable due to their similar chemical properties and genesis. Fe and Mg are iron and steel associations and Ca and Mg are genetically calcophiles and both can be substituted each other. The correlation between Fe and Ca and Mg ($r\sim0.3$) in the mineralised areas could be explained by the fact that calcium and magnesium carbonates are in relation to iron minerals (hematite and goethite). It is also remarkable the low values of $r>0.1$ for Fe and P, and $r\sim0.2$ for Fe and alkaline elements (Na and K).

Other correlations between alkaline and phosphorus with major elements representative of the surrounding rocks where carried out elsewhere (Galán Saunier et al., 2005) for all the

Table 1
Chemical composition expressed in percentage (σ = standard deviation)

TE1

	Depth: 0-56 m 14 samples			Depth: 56–111 m 45 samples			Depth: 111–119 m 5 samples		
	Mean	σ	Min–max	Mean	σ	Min–max	Mean	σ	Min–max
Fe_2O_3	5.33	2.07	2.47–8.93	61.7	7.96	38.0–75.1	11.85	5.82	5.01–19.7
MnO	0.29	0.58	0.03–2.24	2.92	0.65	2.16–6.47	1.01	0.78	0.18–1.95
Al_2O_3	18.4	4.68	10.4–24.4	0.95	0.84	0.19–4.94	20.0	8.53	8.26–27.1
CaO	3.68	4.10	0.01–14.0	3.53	2.71	<0.01–11.3	7.22	7.61	2.10–20.5
MgO	2.77	2.72	0.12–9.08	2.08	1.55	<0.01–6.22	2.80	2.82	1.24–7.83
Na_2O	0.43	0.34	0.03–1.16	0.61	0.43	0.02–1.31	0.54	0.33	0.12–0.95
K_2O	0.70	0.44	0.11–1.44	1.70	3.75	0.14–26.0	0.91	0.51	0.34–1.63
P_2O_5	0.025	0.010	0.014–0.046	0.087	0.046	0.002–0.206	0.036	0.012	0.025–0.055

TE2

	Depth: 0–87 m 24 samples			Depth: 87–93 m 6 samples			Depth: 93–110 m 11 samples		
	Mean	σ	Min–max	Mean	σ	Min–max	Mean	σ	Min–max
Fe_2O_3	6.27	10.6	0.82–52.0	40.2	11.15	22.1–56.3	14.8	10.3	4.84–40.9
MnO	0.27	0.48	<0.01–2.28	1.67	0.43	0.97–2.29	0.69	0.56	0.27–2.28
Al_2O_3	5.38	4.99	0.96–15.1	2.54	0.44	2.08–3.22	1.21	0.74	0.49–2.23
CaO	4.99	7.18	0.21–22.7	1.59	2.84	0.01–7.31	20.0	7.29	7.60–29.8
MgO	3.68	5.43	0.01–18.0	1.56	2.53	0.01–6.61	14.8	2.35	8.21–16.9
Na_2O	0.40	0.55	<0.01–1.68	0.037	0.018	0.020–0.070	0.021	0.011	0.010–0.040
K_2O	0.44	0.60	0.01–1.95	0.047	0.022	0.030–0.090	0.034	0.020	0.010–0.070
P_2O_5	0.028	0.063	0.001–0.320	0.057	0.018	0.037–0.076	0.023	0.010	0.008–0.041

TE3

	Depth: 0–72 m 10 samples			Depth: 72–90 m 19 samples			Depth: 90–114 m 14 samples		
	Mean	σ	Min–max	Mean	σ	Min–max	Mean	σ	Min–max
Fe_2O_3	2.43	2.58	0.76–9.31	51.0	11.5	34–64.3	6.64	2.00	4.32–12.3
MnO	0.08	0.11	0.01–0.34	2.63	0.63	2.2–3.78	0.42	0.21	0.24–1.09
Al_2O_3	1.77	1.06	0.83–4.36	1.32	0.65	0.57–3.02	0.84	0.66	0.19–2.10
CaO	3.85	9.18	0.11–29.8	2.58	5.51	0.01–9.97	26.0	7.85	0.38–30.8
MgO	2.23	5.67	0.01–18.2	2.39	3.25	0.68–2.98	15.7	5.53	0.46–26.4
Na_2O	0.013	0.009	<0.01–0.030	0.023	0.017	<0.001–0.060	0.032	0.023	0.010–0.090
K_2O	0.031	0.012	0.020–0.050	0.035	0.018	<0.001–0.060	0.043	0.028	0.010–0.110
P_2O_5	0.031	0.026	0.009–0.101	0.085	0.076	0.018–0.300	0.015	0.011	0.007–0.046

analysed samples and some examples were represented and explained, being able to clearly distinguish between mineralised and non-mineralised areas.

The ANOVA table decomposes the variance of the data into two components: a between-group component and a within-group component. The *F*-ratio, which in this case equals 1675.57, is a ratio of the between-group estimate to the within-group estimate. Since the *P*-value of the *F*-test is less than 0.05, there is a statistically significant difference between the means of the 8 variables at the 95.0% confidence level. In this sense, a Cluster Analysis for grouping the chemical variables with similar characteristics was carried out in a similar way than for the mineralogical study (Fig. 4B). The results showed only one cluster. It separates in a large distance iron from the other chemical elements which were grouped together.

In order to classify the mineralised samples into three different classes as a function of the three drill holes and to find combinations of the columns which are strongly related to each other, a Discriminant Analysis was made (García Giménez et al., 2005). 71 cases were used to develop a model to discriminate among 3 levels of classes (drill holes). The 8 chemical parameters were entered as predictor variables. The 2 discriminating functions with *P*-values less than 0.05 are statistically significant at the 95% confidence level. Discriminating Functions (F1 and F2) were plotted in the Fig. 7. F1 explains the 91.19% of the total variance and it is a linear combination of the different variables. The most significant standardized coefficients are 1.042 for Ca, −0.973 for Mg, 0.823 for Fe and 0.811 for Na. The remained variance (8.81%) is explained by F2 and it is mainly formed by function coefficients of 0.748 for Mn, −0.445 for Na and 0.335 for P. A visual representation of standardized coefficients of each variable is made in the Fig. 7.

The samples are plotted with different symbols according with their classes. Samples taken in each drill hole are grouped inside an enclosure and they are characterised by a centroid represented by the same symbol in a higher size. This point is the average for each class (unique values in the classification factor field) that uses the discriminant functions. Samples from the three drill holes can be differentiated in groups according with these functions. Samples taken in the mineralised area of TE1 showed the more dispersed points. They could be grouped

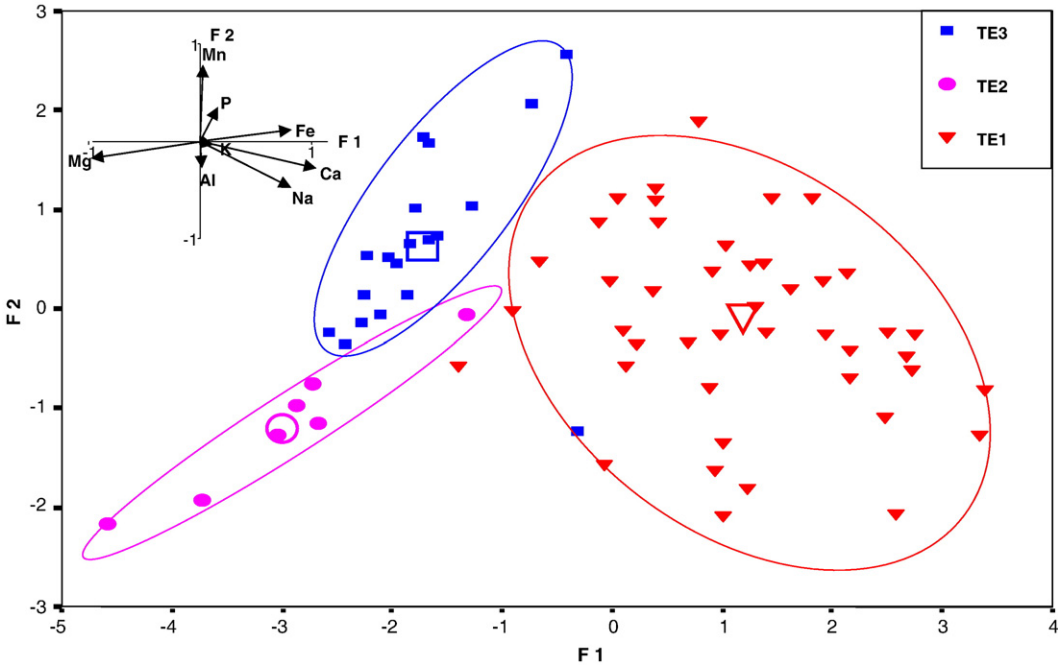

Fig. 7. Linear discriminant analysis of the chemical components.

at values of F1 higher than −1 with elevated level Fe, Na and Ca and large differences in the Ca, Mg and K contents. Samples from TE3 are grouped together at negative values for F1 and values higher than −0.5 for F2. The main variability came from differences in Fe, Mn and Mg composition. In this case, only one sample remains out the group due to its high elevated Ca content. Samples from TE2 could be also grouped at negative values for F1 and F2. In these two latter cases (TE2 and TE3) sample points follow a constant relation between F1 and F2 that allow us an easier grouping.

4.3. Microscopical composition

Fig. 8 represents TE1 vertical chemical composition expressed as percentages of the respective oxides obtained from SEM-EDX data. Taking into account that these data correspond to a punctual analysis (1 μm layers of the some selected samples), these results were in agreement with those obtained from the chemical analyses of the samples for TE1 (Fig. 6). Some differences come from the sample selection and preparation for these analyses. Samples were chosen looking for iron ore particles in order to distinguish better the associated elements to the ore. In these sense, the mineralised area (56–111 m) contained the highest amount of iron and a relative high contents of associated elements such as Mg, Mn and P. In the lower and upper areas pointed up high amounts of Si, Al, K and in a minor extension Mn and P.

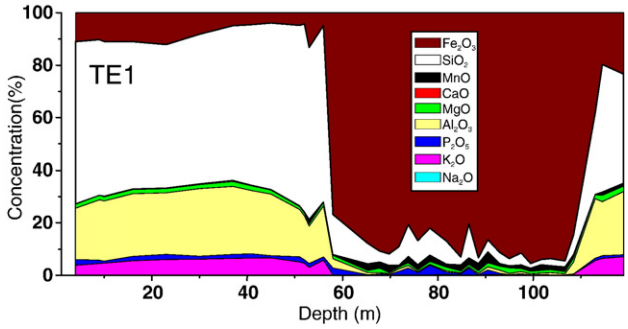

Fig. 8. SEM-EDX analysis: Vertical chemical distribution.

One better geological interpretation of the mineralization can be made from the textural analysis of the different zones. The studied samples came from the mineralised zone of TE1 drill hole. This drill hole is the only one that it was accomplished with complete witness. To accomplish the study, the material is prepared with cronolite to facilitate preparations and manipulations of thin sections. That permitted the study of the distribution and characteristics of present minerals.

Fig. 9 A and B are photomicrographs obtaining from Polarisation and Scanning Electron Microscopies respectively, corresponding to samples governed by a massive mineralization. These samples show representative textures of different stages of the mineralization evolution, in the following sequence:

1) Filling joint texture, related to replacement on cleavage planes of carbonates. It was probably produced “in situ”. In certain samples very compact and small splits, that you could fill, frequently appear. Among them, it can be distinguished trainings with grating appearance (Fig. 9–A1). The irregular formations are associated with glomerular textures, penetrating frequently inside due to a subsequent stage to the glomerular training. When they were analyzed with detail (Fig. 9–B1), these lattice works was proven to be aligned crystal trainings of pseudoprismatic hematite alternating with small porous.

2) Banded texture: this texture is formed with rounded small size particles of about 0.2 μm that are grouped in the form of defaults whose size grows as the depth of the mineralization increases and that suppose a recrystallization phenomenon from gels. In addition, this texture shows a sequence of different colour levels (reddish to yellow) produced by mechanical deformations that impacted on the materials in a plastic phase (Fig. 9-A2). These layers, observed by SEM, show the presence of porous materials with different morphologies and chaotic distribution; such as globular aggregates constituted by particles between 0.2 and 1 μm sizes. These materials are partially recrystallised as goethite, which have average sizes between 2–3 μm with irregular contours and a laminate aspect (Fig. 9-B2).

In the composition of these botryoidal aggregates emphasizes the high Mn and Si contents, coinciding with the high phosphorus concentrations in the samples. From the great porosity of these samples and the cottoned aspect of the globular aggregates, it could be concluded that it would be an initial crystallization phase.

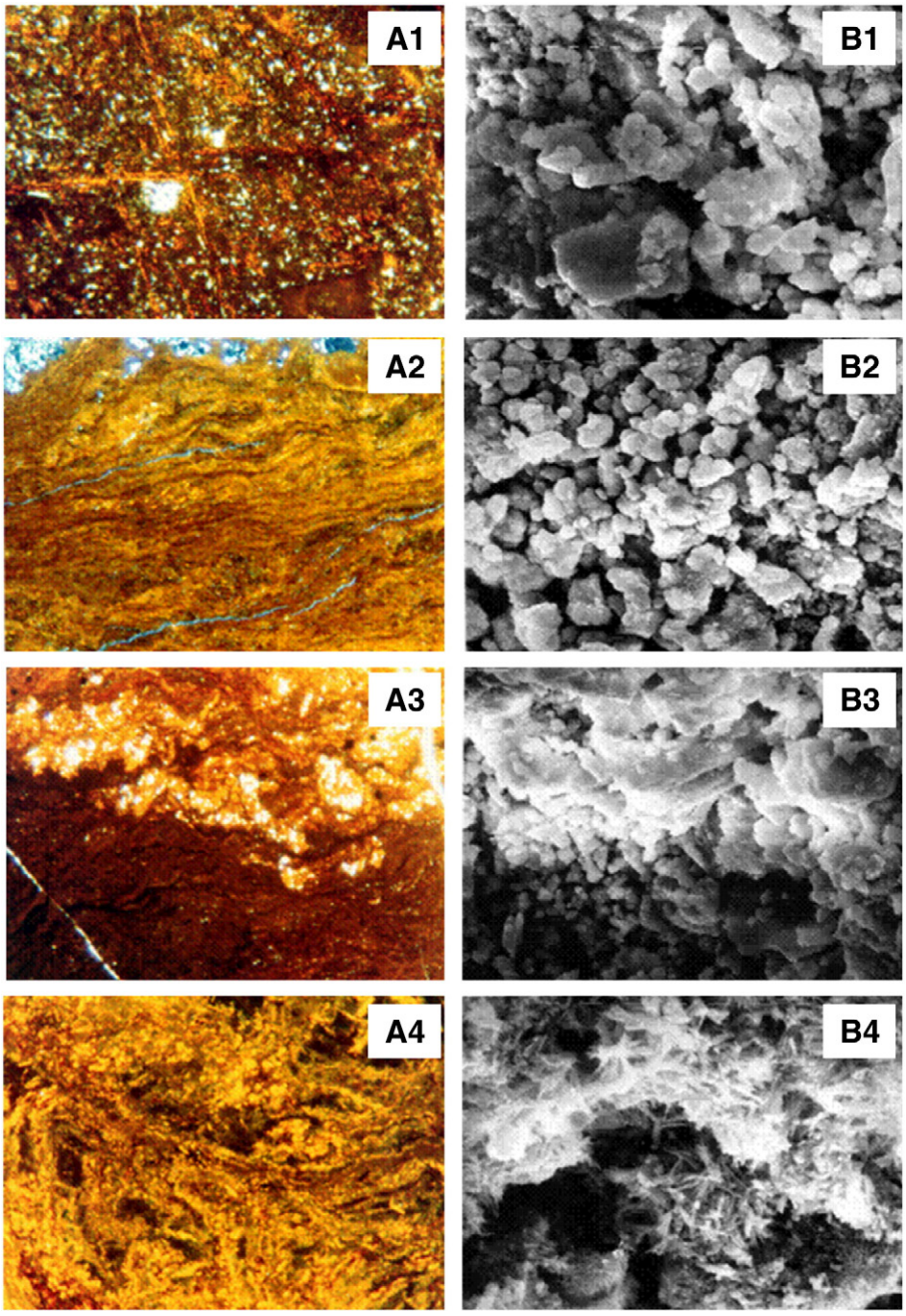

Fig. 9. Photomicrographs of A. Polarisation microscopy, crossed nicols: A1. Panoramic general of the fissures in the form of latticework (X125). A2. Banded textures (X16). A3. Diagenetic transformation of banded textures (X16). A4. Glomerular texture (X40). B. Scanning electron microscopy (SEM): B1. Detail of the pseudoprismatic forms in the fissures (×2500). B2. Detail of the bands with mineral of various nature (×2500). B3. Detail of the contact between banded and laminar textures (×2500). B4. Detail of the needled aggregates of goethite (×5000).

Comparing the characteristics of the factory of these samples with the corresponding XRD analyses, it could be related small size globular forms to chemical composition close to limonite, where goethite and hematite phases coexist.

3) Laminar texture: it is the recrystallization result from the banded texture. The banded textures with fine lamination frequently become most homogeneous textures losing the initial banded and the plates take the aspect of saw tooth (Fig. 9-A3). By SEM it could be observed pseudoprismatic crystals of hematite with sizes close to 10 μm, which are orientated in planes forming a laminar structure (Fig. 9-B3).
4) Glomerular texture, related to the collapse phenomena of the karstic cavity that can affect to anyone of the textures before described. It shows zones with remains of the bands described before mechanically distorted. They have the appearance of glomerular materials by polarization microscope observations (Fig. 9-A4). By SEM it could be observed compact masses, with denser zones corresponding to hematite alternating with hollows draped by growing radial aggregates with acicular crystals of goethite of average sizes between 2 and 3 μm (Fig. 9-B4).

In general, we could say that the powdered character of the mineralization is due to the existence of small particles (0.2–3.0 μm) with an incipient degree of crystallization and low cohesion among them. On the other hand, the subaerial character of the mineralization together with its high porosity and the predominance of hemihydrated phases (goethite) over anhydrous phases (hematite) would be indicative of deposition conditions later to metamorphism stages (Fernández Nieto et al., 1981) dating the age of karstification in the Middle Pliocene.

5. Conclusions

A suitable combination of the physicochemical and chemometric analytical techniques used for mine profitability studies provides useful information about geological, mineralogical and chemical composition of samples corresponding to different depths of the three studied drill holes (TE1, TE2 and TE3). Statistical and chemometrical tools such as correlation, cluster and discriminant analysis and box and whiskers graphics constitute an important help in the interpretation of those analysis results and in the deduction of clear and objective conclusions. Data obtained from all these analytical techniques are in good agreement and provide the way to obtain a blend of market saleable quality products. Results showed an abundant presence of iron ore in TE1 (56–11 m), where the highest mean percentage in the iron content (61.7%) was found, with a maximum value of 75.1%, being TE2 the least mineralised with an average content of iron about 40.2%. TE1 was the drill hole with the highest grade of mineralization, but at the same time presented the highest amounts of Na, K and P associated to the iron ore, together with Al, Ca and Mn. In the mineralised area of TE1, phosphorus average content were 0.087% P_2O_5, but in some particular samples this value was above the recommended 0.15%, but never between 65 and 95 m deep. However the contents of K_2O+Na_2O in most of the samples were above 0.55%. Mineralised areas in TE2 (87–93 m) and TE3 (72–90 m) had a minor extension, but K_2O+Na_2O contents always were under 0.16% and 0.12% values respectively (below the maximum value recommended), while P_2O_5 average contents were 0.057% and 0.085% for TE2 and TE3 respectively. In TE2 all the samples showed P_2O_5 values below 0.08% and in TE3 only two samples of twenty showed values of P_2O_5 above 0.15% recommended. It can be also concluded that Na and K were in a close relation to micaceous minerals from slates like muscovite and paragonite and in a minor proportion to feldspars associated to quartzite. On the other hand, P was in close relation to Mg-Ca carbonates, iron oxides and iron hydroxides like ferrihidrite, goethite an in a minor extension to hematite. According to Sholkovitz et al., 1989, the presence of reefs in the surroundings of the mineralization could be a primary source of phosphorus.

All these studies show the use of a suitable methodology for the treatment of a large number of data coming from different analytical techniques helped by several statistical tools. They provide wide information of several aspects (chemistry, geology, mineralogy, morphology, etc.) of the subject under study. This methodology could be applied in a similar way to different topics in the chemical and geological fields.

References

Barahona, E., 1974. Arcillas de ladrillería de la provincia de Granada. Evaluación de algunos ensayos en materias primas. Doctoral Dissertation, Universidad de Granada.

Brindley, G.W., 1980. Order-disorder in clay minerals structure. In: Bridley, G.W., Brown, G. (Eds.), Cristal Structures of Clays Minerals and their X-Ray identification. Mineralogical Society Monograph, vol. 5. London, 496 pp.

Fernández Nieto, C., 1977. Mineralogía y mineralogénesis del yacimiento de hierro de Ojos Negros. Doctoral Dissertation, Spain, Univ. Zaragoza, 250 pp.

Fernández Nieto, C., Arrese, F., 1979. Mineralogía y mineralógenesis del yacimiento de hierro de Ojos Negros (Teruel y Guadalajara), I Reunión de Miner. Metal. del hierro, Temas Geol. Min. Madrid, Spain, I.G.M.E. 3, 139–177.

Fernández-Nieto, C., Fernández Rubio, R., Gutiérrez Elorza, M., Arrese Serrano, F., 1981. Papel de la karstificación en la génesis de los yacimientos de hierro de Sierra Menera (Teruel y Guadalajara). Boletin Geologico y Minero 92 (2), 127–140.

Fernández Nieto, C., Torres Ruiz, J., Subias Perez, I., Faulo Gonzalez, I., Gonzalez Lopez, J.M., 2003. Genesis of Mg–Fe carbonates from the Sierra Menera magnesitesiderite deposits, Northeast Spain: evidence from fluid inclusions, trace elements, rare earth elements, and stable isotope data. Economic Geology 98, 1413–1426.

Fernández Rubio, R., 1976. Características geológicas de las Minas de Ojos Negros, X Curso de geología Práctica, Teruel. 36 pp.

Galán Saunier, A., Petit Domínguez, M.D., Rucandio, I., García Giménez, R., 2005. Study of toxic elements in iron ores from the Ojos Negros Disctric (Teruel, Spain). Proceedings of the 9th Internacional Mine Water Congress, pp. 661–667.

García Giménez, R., Vigil de la Villa, R., Recio de la Rosa, P., Petit Domínguez, M.D., Rucandio, M.I., 2005. Analytical and multivariate study of roman age architectural terracotta from northeast of Spain. Talanta 65, 861–868.

García Giménez, R., Vigil de la Villa, R., Petit Domínguez, M.D., Rucandio, M.I., 2006. Application of chemical, physical and chemometric analytical techniques to the study of ancient ceramic oil lamps. Talanta 68, 1236–1246.

Haygarth, P.M., 2005. Linking landscape sources of phosphorus and sediment to ecological impacts in surface waters. Science of the Total Environment 344, 1–3.

Haygarth, P.M., Condron, L.M., Heathwaite, A.L., Turner, B.L., Harris, G.P., 2005. The phosphorus transfer continuum: linking sources to impact with an interdisciplinary and multiscaled approach. Science of the Total Environment 344, 5–14.

Herranz, P., Gutiérrez Marco, J.C., Pieren Pidal, A.P., Robardet, M., San José Lancha, M.A., Rábano, I., Sarmiento, G.N., 2003. The Ordovician succession from the western Iberian Ranges (NE Spain): a review with new data. Insugeo 17, 417–424.

Hoft, D., Oxman, J., Rogers, C., 1979. Direct determination of phosphorus in fertilizers by atomic absorption spectroscopy. Journal of Agricultural and Food Chemistry 27, 145–147.

Jackson, M.L., 1976. Análisis químico de suelos, 3rd ed. Omega.

Kirkbright, G.F., Ward, A.F., West, T.S., 1972. The determination of sulphur and phosphorus by atomic emission spectrometry with an induction-coupled high-frequency plasma source. Analytica Chimica Acta 62, 241–251.

Marini, F., Magrì, A.L., Balestrieri, F., Fabretti, F., Marini, D., 2004. Supervised pattern recognition applied to the discrimination of the floral origin of six types of Italian hpney samples. Analytica Chimica Acta 515, 117–125.

Papadopoulou, D.N., Zachariadis, G.A., Anthemidis, A.N., Tsirliganis, N.C., Straits, J.A., 2004. Micro-XRF analysis of ancient ceramics that exhibit color variations in their lateral cross-section. 34th International Symposium on Archaeometry. Zaragoza. Spain.

Pereira, A.M.T., Brandao, P.R.G., 2001. Statistical validation of standardless and standard-based analysis by X-ray fluorescence spectrometry in iron ores characterization. Minerals Engineering 14, 1659–1670.

Schultz, L.G., 1964. Quantitative interpretation of the mineralogical composition from X-ray and Chemical data for the Pierre Shale. U.S. Geological Survey Professional Paper 391 C, 31 pp.

Sholkovitz, E.R., Piepgras, D.J., Jacobsen, S.B., 1989. The pore water chemistry of rare earth elements in Buzzard Bay sediments. Geochimica et Cosmochimica Acta 53 (11), 2847–2856.

Urquiza, A., Garcia, R., Pozo, M., Leguey, S., 1985. Estudio mineralógico y textural de las mineralizaciones de hierro de la zona "Tío Elías" del yacimiento de Ojos Negros (Teruel). Boletin Sociedad Espanola de Mineralogia 145–155.

Villena, J., 1976. Estudio geológico del sector de las cadenas Ibéricas comprendido entre Molina de Aragón y Monreal (provincias de Guadalajara y Teruel). Boletin Geologico y Minero 87, 329–354.

Zitzmann, A., Newman Redlin, C., 1976. The iron ore deposits of Spain. In: Walter, H.W., Zitmann, A. (Eds.), The iron deposits of Europe and adjacent area. Hannover, Bundesanstalt für Geowissenschaften und Rohstoffe, vol. 1, pp. 269–278.